Supplementary Information

Cu NPs doped d-NH_2-MIL-125 for Light-Driven Hydrogen Evolution

Mingyang Sun , Fengyang Yu , Jinfeng Wang, Yao Wang, Xu Jing* and Chunying Duan

State Key Laboratory of Fine Chemicals, Zhang Dayu College of Chemistry, Dalian University of Technology, Dalian, 116024, P. R. China

Corresponding Authors

* E-mail: xjing@dlut.edu.cn

Contents

1. Materials and Equipments

All chemical reagents were commercially available and used without further purification. The size, microstructure, and morphology of NH_2-MIL-125, d-NH_2-MIL-125, Cu/ d-NH_2-MIL-125, and CuNPs/d-NH_2-MIL-125 with different amounts of CuNPs were investigated by using transmission electron microscopy (TEM) and scanning electron microscopy (SEM) on Tecnai F30. X-ray diffraction (XRD) was were obtained on Rigaku D/Max 2400 automatic powder X-ray diffractometer with Cu-Kα radiation (λ= 1.5418 Å). UV-vis diffuse reflectance data were recorded on a HITACHI U-4100 spectrometer in the wavelength range of 200-800 nm and a white standard of $BaSO_4$ was used as a reference. Electrochemical/photoelectrochemical measurements were carried out on a CHI660C electrochemical workstation with a conventional three-electrode cell. Electron paramagnetic resonance (EPR) spectrum was conducted on Bruker A200 at room temperature. The contents of Cu in the hybrid materials were quantified by inductively coupled plasma atomic emission spectroscopy (ICP-AES) on Optima 2000DV. The gas products were analyzed and identified by gas chromatography (GC7900 Techcomp). The liquid products were analyzed the GC (Shimadzu GC-2014C).

2. Experimental Section

Synthesis of NH_2-MIL-125

In a typical method, the linker H_2ATA (217 mg) was dissolved in 5.0 mL of DMF and 5.0 mL of MeOH and stirred at room temperature for about 10 min. Then, 0.177 mL of isopropyl titanate was added to the mixture and sonicated for 5 min. Following that, the mixture was transfered into a 15 mL Teflon-lined stainless autoclave and react at 150 °C for 15 h. Production was collected by centrifugation and washed for three times with DMF and methanol. Finally, NH_2-MIL-125 was activated by removing the solvent under vacuum for 12 h at 70 °C.

Synthesis of d-NH_2-MIL-125

As-prepared NH_2-MIL-125(400 mg) were dispersed into 200 mL EtOH with 100 μl HF under ultrasonic treatment for 1 min, then stirred for 2 hours. The obtained yellow powder was washed several times with EtOH and dried under vacuum for 12 h at 70 °C. The sample then was dried to afford the bright yellow solid product.

Synthesis of Cu/d-NH_2-MIL-125

The synthesis process of a series of Cu/d-NH_2-MIL-125 was described as follows. A suspension containing d-NH_2-MIL-125 (50 mg),0.053 mM $Cu(NO_3)_2$, DMF solution (0.5 ml), and methanol (20 mL) was ultrasonic for 2 h, the obtained precipitate was separated by centrifugation, washed repeatedly with methanol. The Cu contents were confirmed by inductively coupled plasma (ICP) analysis.

Synthesis of CuNPs/d-NH_2-MIL-125

As-prepared Cu/d-NH_2-MIL-125 were thermal treated at 250 °C for 2 h in a quartz tube furnace under H_2/Ar(5:95) atmosphere with a ramp rate of 2 °C min^{-1} to achieve the 2 wt% CuNPs/d-NH_2-MIL-125, To prepare the 1 wt% CuNPs/d-NH_2-MIL-125 and 4 wt% CuNPs/d-NH_2-MIL-125, the addition amounts of $Cu(NO_3)_2$ solution were changed to 0.026 mM and 0.106 mM in DMF with no change in other steps.

Photoelectrochemical measurement

Photoelectrochemical measurements were performed on a standard three-electrode system, in single-compartment quartz cell, photocatalysts electrode as the working electrode, Ag/AgCl electrode as a reference electrode, and Pt slice as the counter electrode. A 300 W Xe lamp with UV cut-off filter ($\lambda > 420$ nm, 10 mW cm^{-2}) was used as the light source of photocurrent tests and Mott-Schottky plots in 3.5M KCl aqueous solution. The as-prepared samples (1 mg) were dispersed into 0.1 mL mixture (V_{H_2O}/V_{EtOH}=1/1) with 10 μL Nafion and then the suspension (50 μl) were dropped onto the surface of a FTO plate (1mg cm^{-2} catalyst film on 2 cm^{-2} FTO). The prepared working electrode was dried by IR lamp.

Photocatalytic Activity Evaluation

Photocatalytic hydrogen evolution experiments were performed under irradiation of a 300 W Xe lamp with a UV cut-off filter (>420 nm,10 mW cm^{-2}),3 mg of catalyst, 4 mL of CH_3CN, 1 mL of deionized water, and 200 μL of TEOA were added in a 25 mL optical reaction vessel. Next, the reaction system was thoroughly degassed with Ar for over 20 min. The reactor was irradiated by the Xe lamp, the temperature was controlled by circulation cooling water and the suspension was stirred. The gas product was measured by a gas chromatography (GC7900 Techcomp) equipped with a thermal conductivity detector (TCD). 1 mL syringe was used to extract gas of reaction system and injected into the GC for each measurement of H_2 generation.

Photocatalytic oxidation and reduction coupling reaction was performed under 405 nm LED (100 W) as the light source, 3 mg of catalyst, 2 mL of DMF, 300 μL of H_2O,30 μL tetrahydroisoquinoline were added in a 25 ml optical reaction vessel with no change in other steps. Liquid product was analyzed by the GC (Shimadzu GC-2014C) with a flame ionization detector (FID) and dodecane was added as an internal standard.

Mott-Schottky measurement

The Mott–Schottky plots were determined to obtain the flat-band potential and carrier density. In addition, the capacitance measurement was performed on the electrode/electrolyte according to the Mott-Schottky equation.

$$\frac{1}{C^2} = \frac{2}{N_d e \varepsilon \varepsilon_0}\left(E - E_{FB} - \frac{KT}{e}\right)$$

Where C is the space charge capacitance in the semiconductor, N_d is the electron carrier density, e is the elemental charge, ε_0 is the permittivity of a vacuum, ε is the relative permittivity of the semiconductor, E is the applied potential, E_{FB} is the flat band potential, T is the temperature, and k is the Boltzmann constant.

3. Characterization of NH_2-MIL-125, d-NH_2-MIL-125, Cu/d-NH_2-MIL-125, and CuNPs/d-NH_2-MIL-125

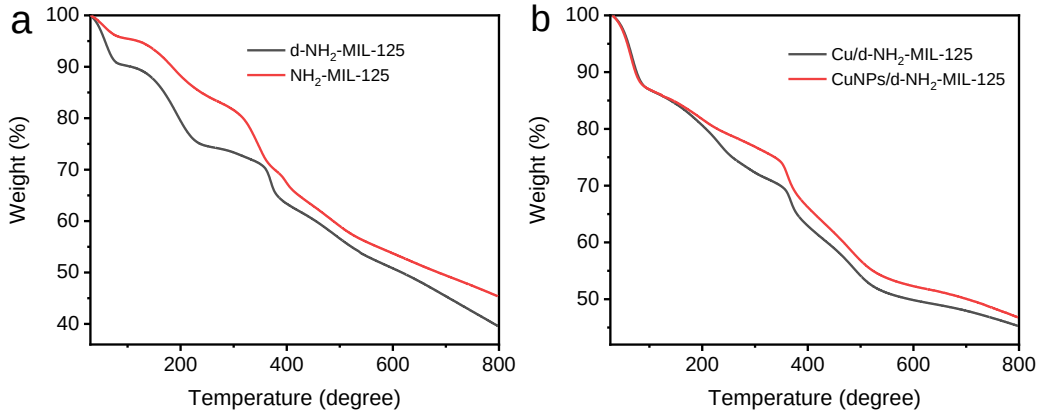

Figure S1. TG pattern of (a)NH_2-MIL-125 and d-NH_2-MIL-125, (b)Cu/d-NH_2-MIL-125 and CuNPs/d-NH_2-MIL-125.

The pore of d-NH_2-MIL-125 contains more DMF. At 150 °C-350 °C, it is the residual DMF combustion in the MOFs pore. A higher weight loss of d-NH_2-MIL-125 after thermal decomposition of organics demonstrate Ti cluster was resolved by acid treatment. Major weight loss between 350 °C and 600 °C is corresponding to Organic linker burned, which demonstrate the stability of d-NH_2-MIL-125, CuNPs/d-NH_2-MIL-125 and Cu/d-NH_2-MIL-125.

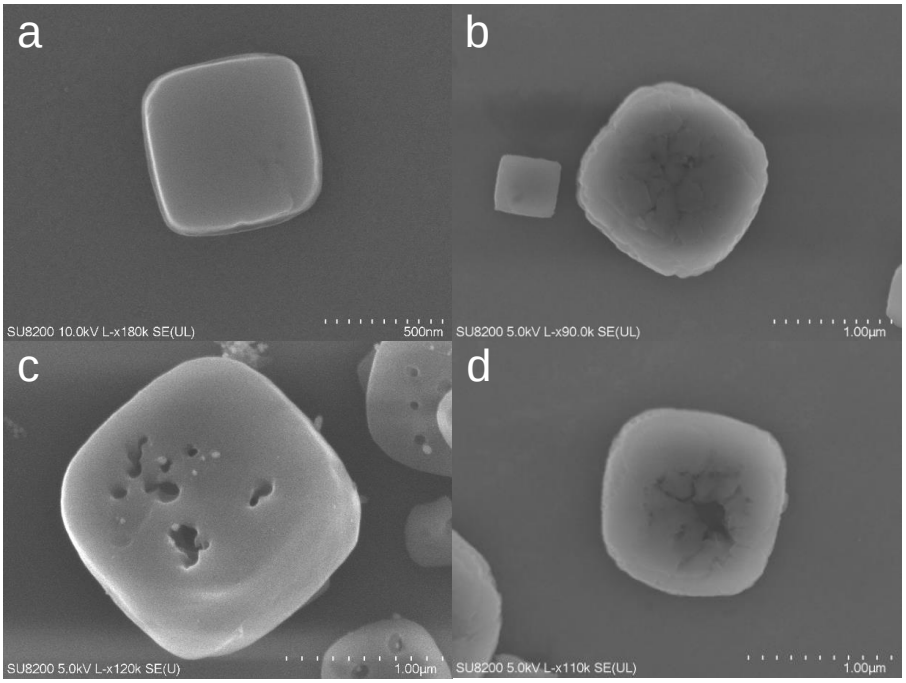

Figure S2. SEM image of (a) NH_2-MIL-125, (b) d-NH_2-MIL-125, (c) CuNPs/d-NH_2-MIL-125, (d) Cu/d-NH_2-MIL-125.

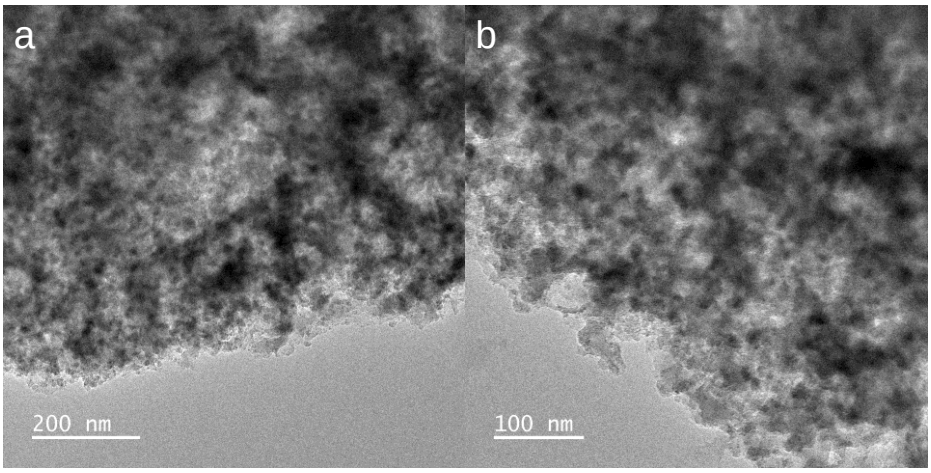

Figure S3. TEM images of 2wt% CuNPs/d-NH_2-MIL-125 composite. Scale bar, (a)200nm, (b)100 nm.

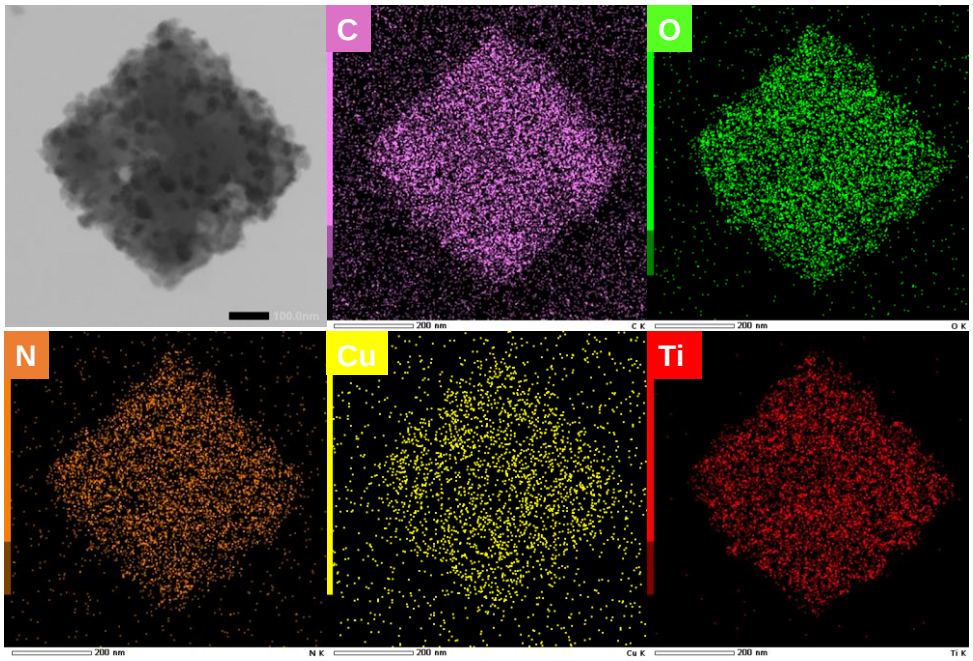

Figure S4. TEM image and element mapping images of 4 wt%CuNPs/d-NH_2-MIL-125.

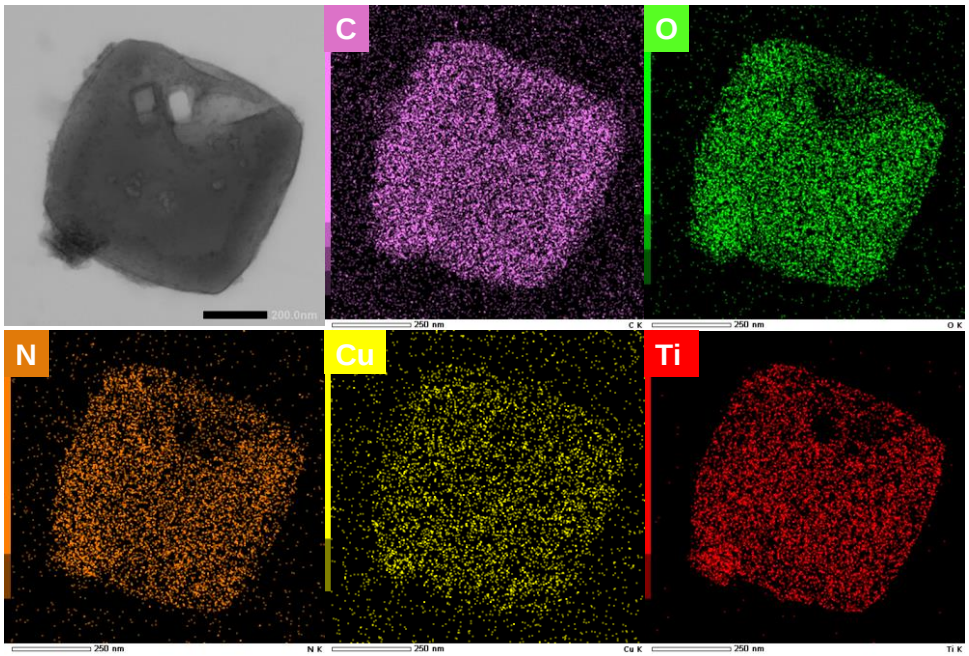

Figure S5. TEM image and element mapping images of Cu/d-NH_2-MIL-125.

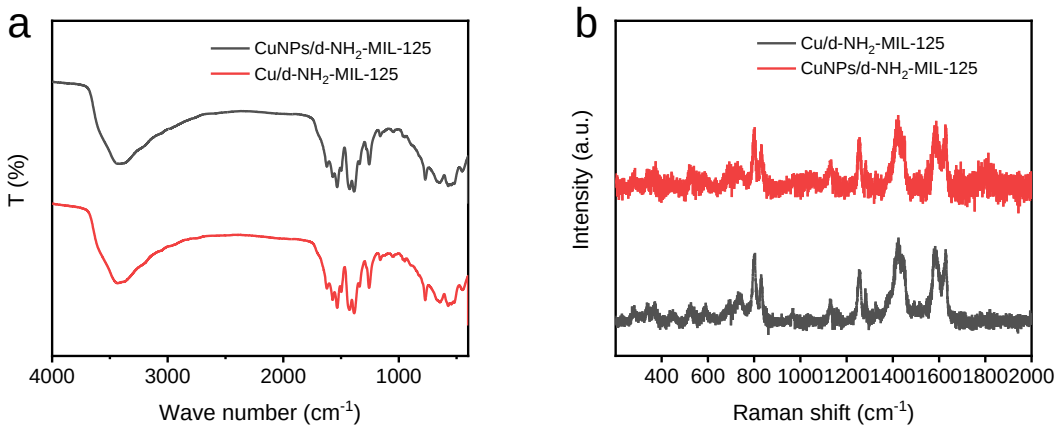

Figure S6. (a) FT-IR spectra of Cu/d-NH_2-MIL-125 and CuNPs/d-NH_2-MIL-125. (b) Raman spectra of Cu/d-NH_2-MIL-125 and CuNPs/d-NH_2-MIL-125.

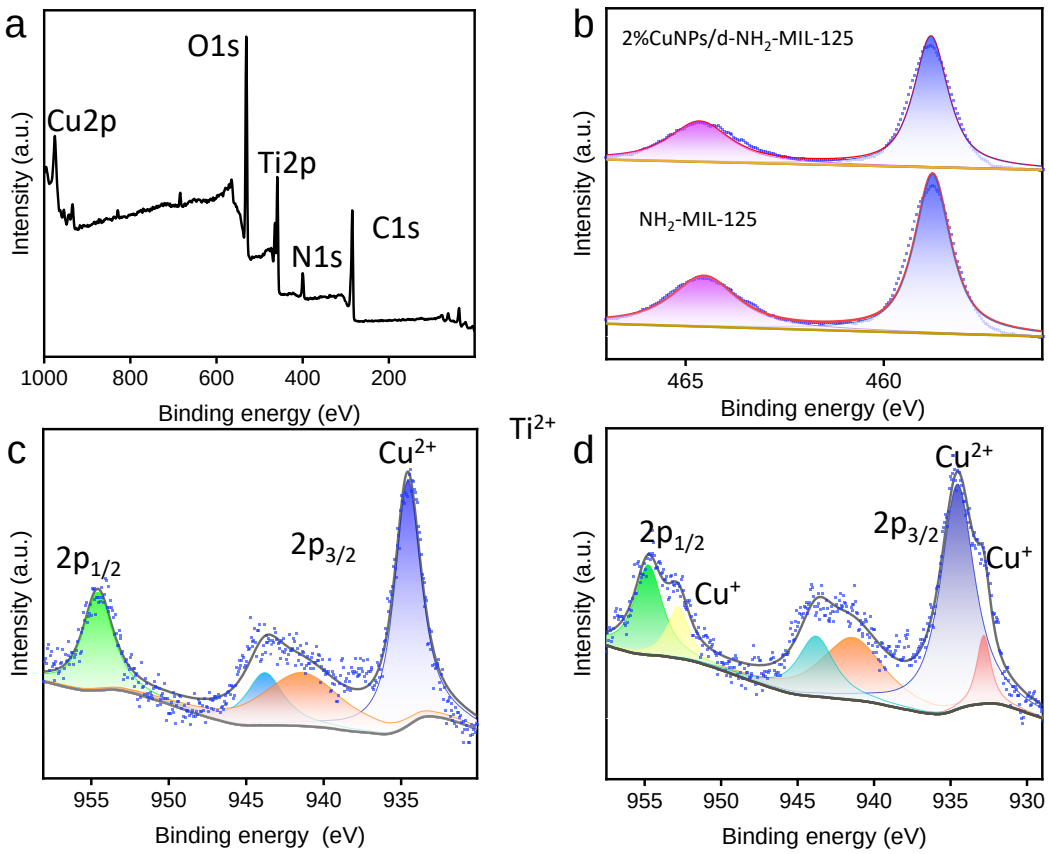

Figure S7. (a) XPS analysis for CuNPs/d-NH_2-MIL-125 Cu2p (b) Ti 2p, (c) Cu2p of the Cu/d-NH_2-MIL-125 (d) Cu2p of the CuNPs/d-NH_2-MIL-125

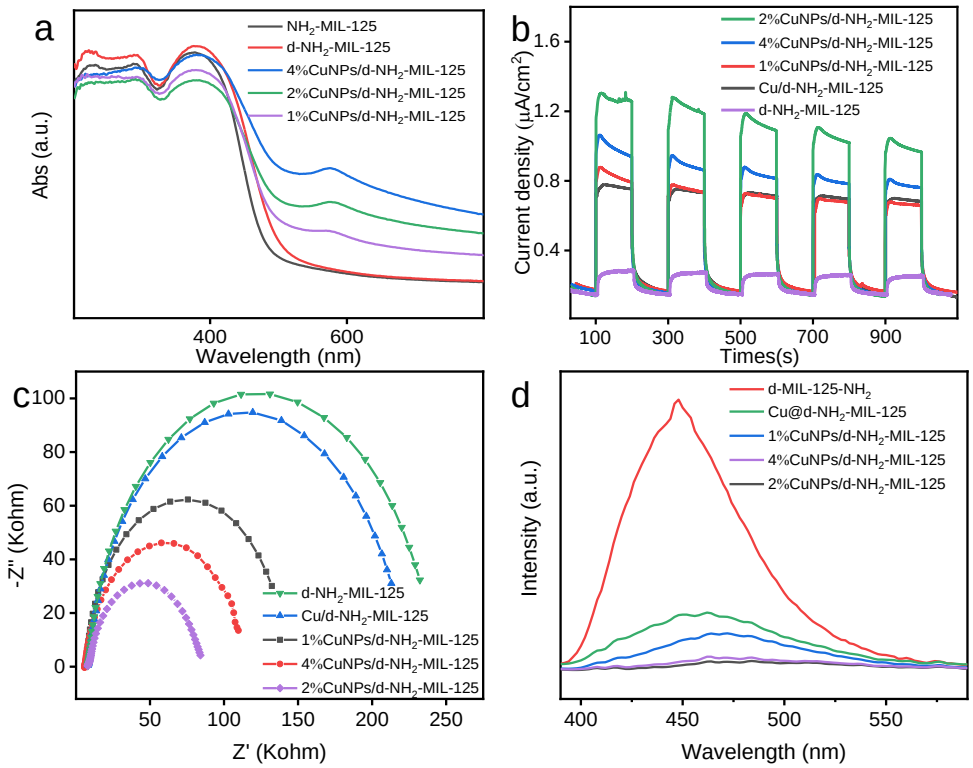

Figure S8. (a) UV-vis diffuse reflectance spectra (b) Transient photocurrent representation, (c) EIS Nyquist plots and (d) PL spectra of d-NH_2-MIL-125, Cu/d-NH_2-MIL-125 and CuNPs/d-NH_2-MIL-125 nanohybrids with different loading amounts of Cu NPs.

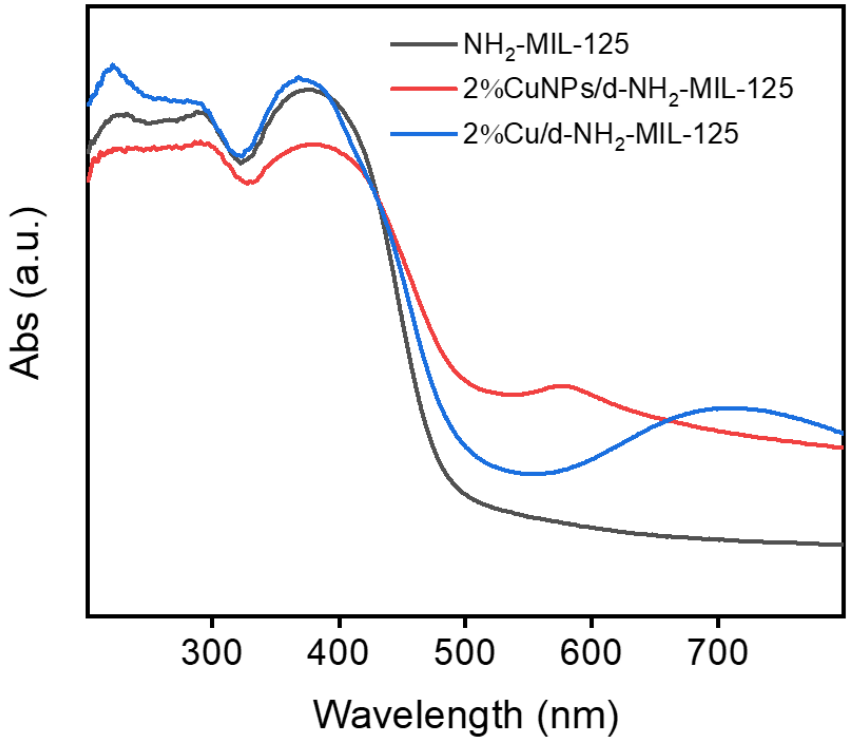

Figure S9. UV-Vis of NH_2-MIL-125, 2 wt%CuNPs/d-NH_2-MIL-125, Cu/d-NH_2-MIL-125.

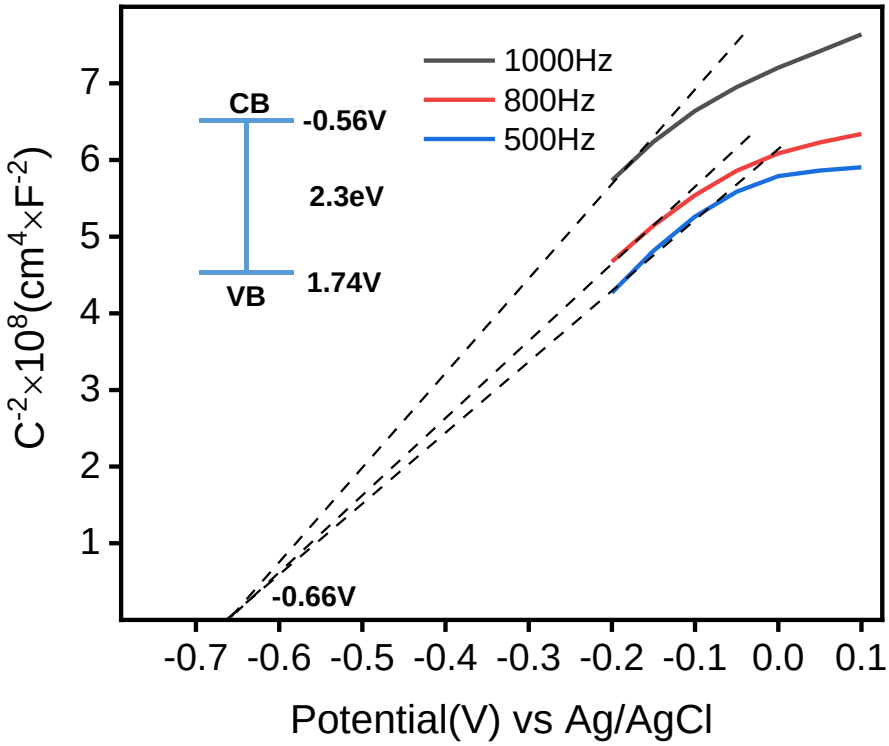

Figure S10. The Mott-Schottky plots, CB (inset), VB (inset), and band gaps (inset) of 2 wt%CuNPs/d-NH_2-MIL-125.

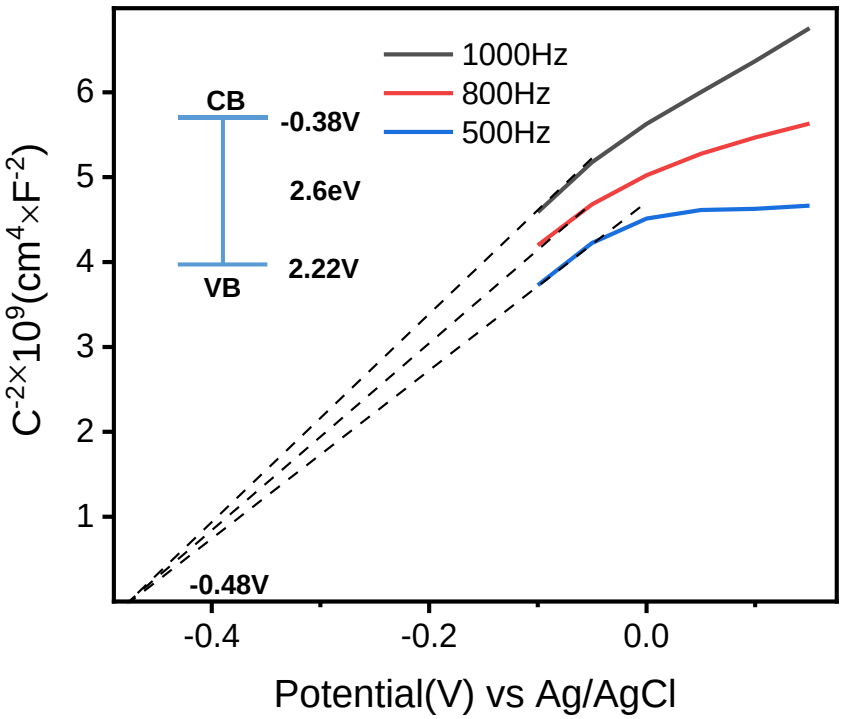

Figure S11. The Mott-Schottky plots, CB (inset), VB (inset), and band gaps (inset) of NH_2-MIL-125.

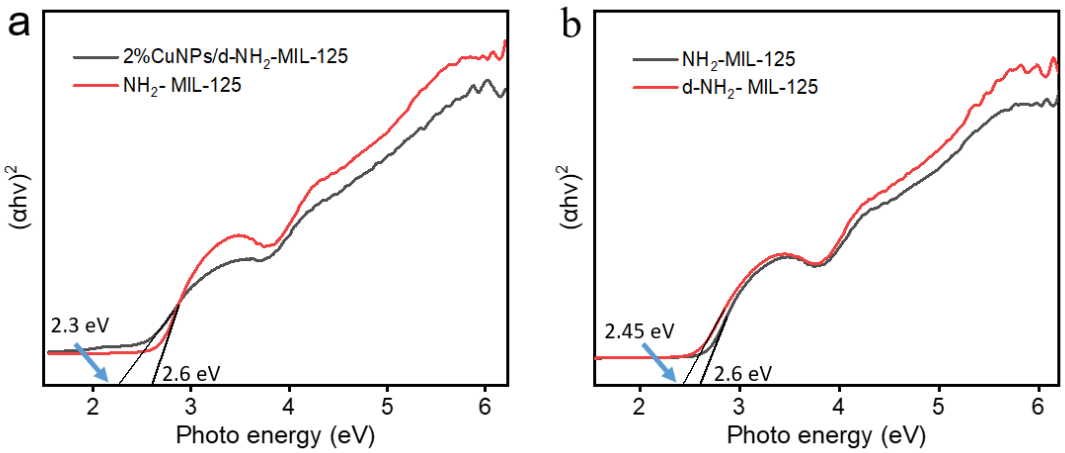

Figure S12. Energy band gaps of (a) 2 wt%CuNPs/d-NH_2-MIL-125 and (b) d-NH_2-MIL-125.

4. Photocatalytic Details Mediated by CuNPs/d-NH_2-MIL-125

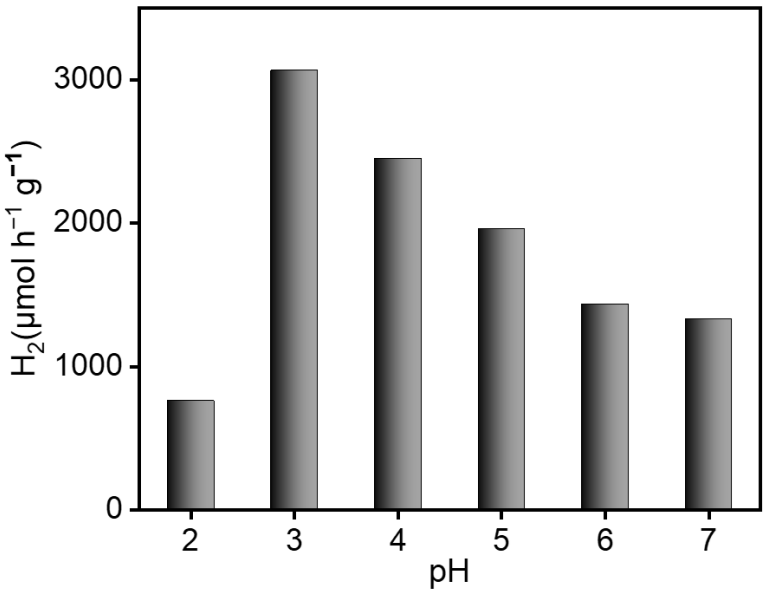

Figure S13. Photocatalytic hydrogen production amounts on the different pH.

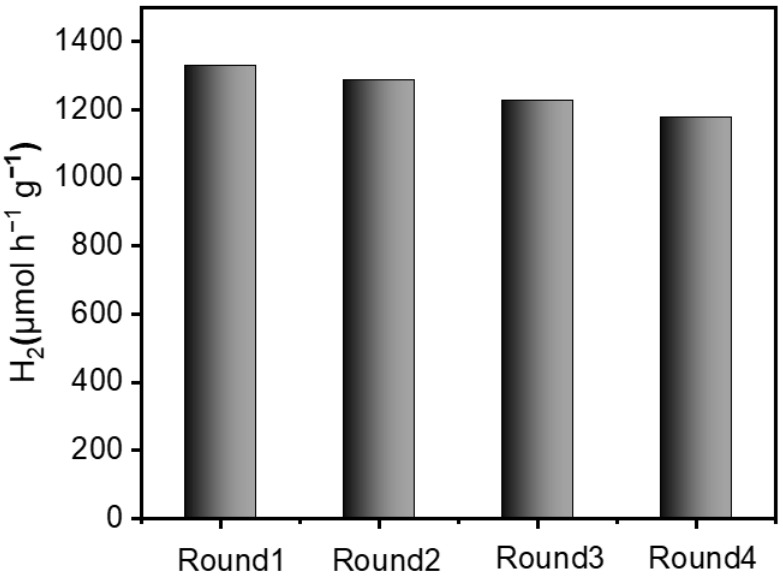

Figure S14. Photocatalytic stability of 2 wt%CuNPs/d-NH_2-MIL-125 during photocatalytic cycles.

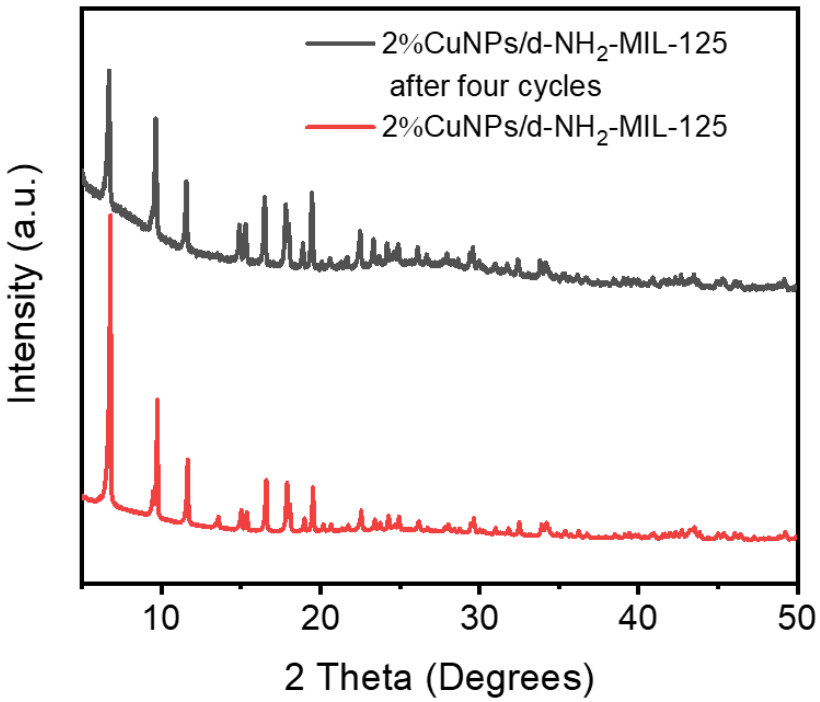

Figure S15. XRD pattern of 2 wt% CuNPs/d-NH_2-MIL-125 after four-cycle photocatalytic dehydrogenation and the as-synthesized 2 wt% CuNPs/d-NH_2-MIL-125.

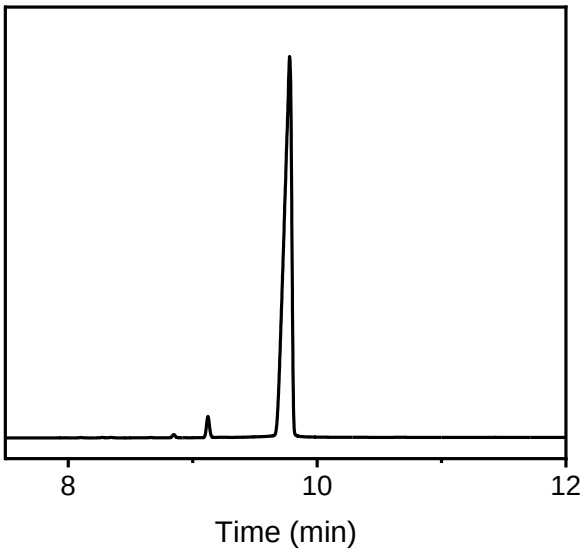

Figure S16. GC spectrum of the reaction mixture after photocatalytic tetrahydroisoquinoline in H_2O/DMF.

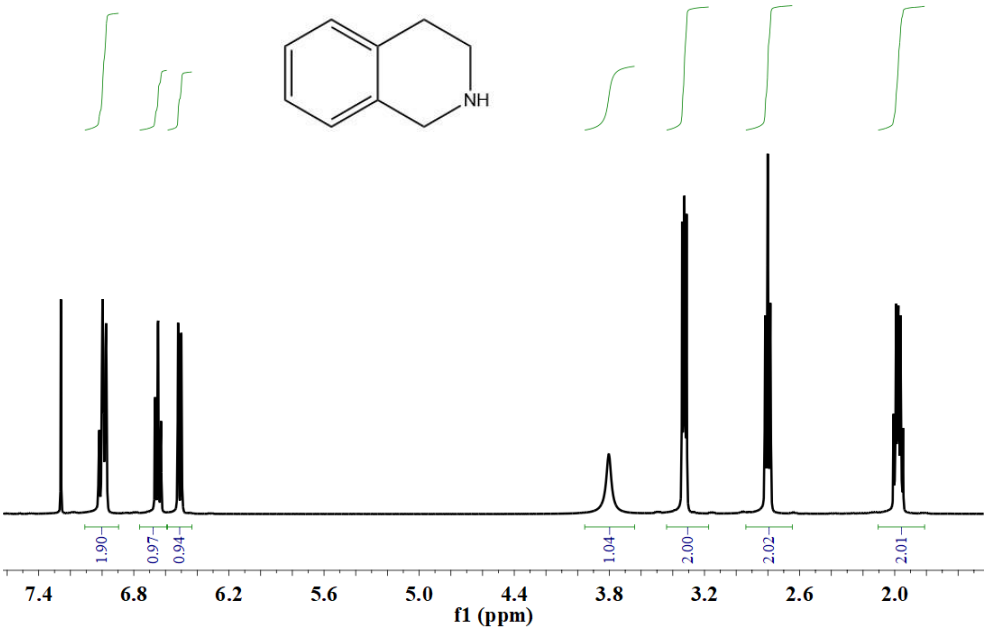

^{1}H NMR (400 MHz, $CDCl_3$) δ 7.16 –7.10 (m, 2H), 7.09 (dd, J = 8.4, 4.4 Hz, 1H),7.03–6.99 (m, 1H), 4.01 (s, 2H), 3.14 (t, J = 6.0 Hz, 2H), 2.80 (t, J = 6.0Hz, 2H), 1.76 (s, 1H).

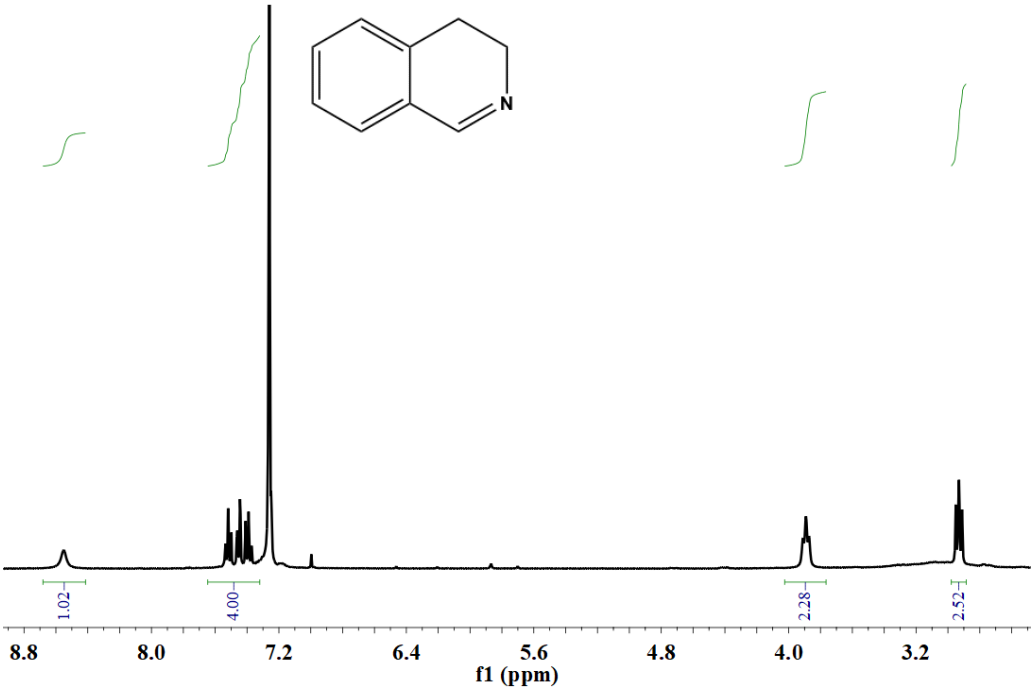

^{1}H NMR ($CDCl_3$, 400 MHz) δ 8.34 (t, J =2.0 Hz, 1H), 7.38-7.28 (m, 3H), 7.16 (d, J =7.3 Hz, 1H), 3.80-3.76 (m, 2H), 2.76 (t, J= 7.9 Hz, 2H).

5. Exploration of Reaction Mechanism

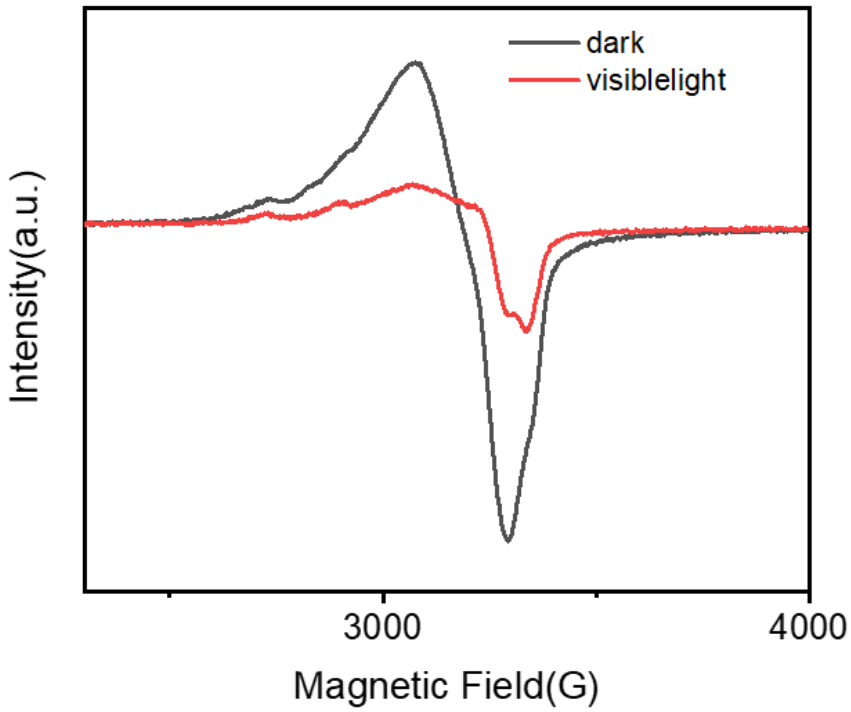

Figure S17. Low-temperature X-band EPR spectra of 2 wt% CuNPs/d-NH_2-MIL-125 under different conditions.

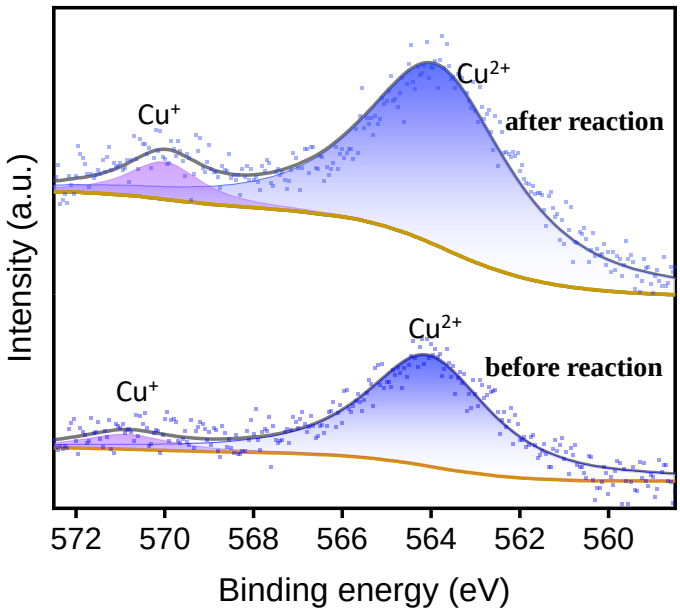

Figure S18. The Auger Cu LMM spectra of the 2 wt% CuNPs/d-NH_2-MIL-125 before and after the photocatalytic reaction.

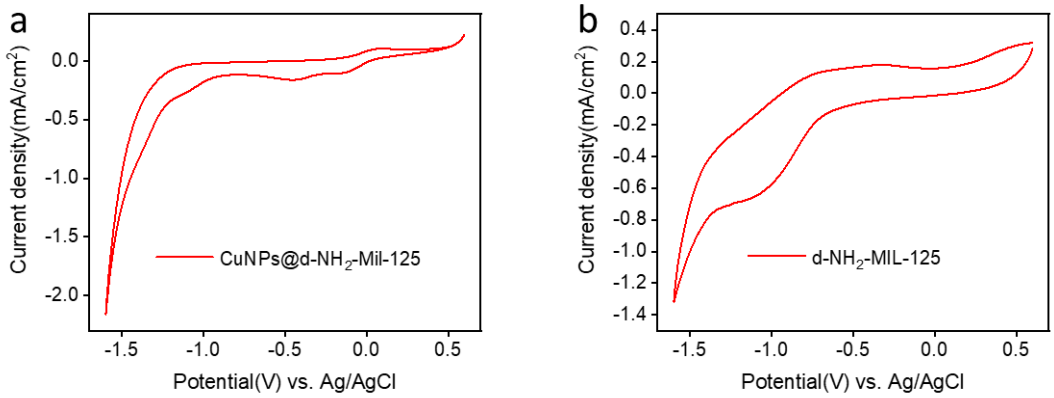

Figure S19. The cyclic voltammograms (a) 2 wt% CuNPs/d-NH_2-MIL-125 and (b) d-NH_2-MIL-125.

Table S1. ICP results for Cu contents in 1 wt% CuNPs/d-NH_2-MIL-125, 2 wt% CuNPs/d-NH_2-MIL-125, 4 wt% CuNPs/d-NH_2-MIL-125, Cu/d-NH_2-MIL-125.

catalyst	content
1 wt%CuNPs/d-NH_2-MIL-125	0.97 wt%
2 wt%CuNPs/d-NH_2-MIL-125	2.14 wt%
4 wt%CuNPs/d-NH_2-MIL-125	4.28 wt%
Cu/d-NH_2-MIL-125	2.03 wt%

Table S2. Photocatalytic activity of some typical MOFs catalysts for hydrogen production.

Photocatalyst	Condition	Activity ($\mu mol \cdot g^{-1} \cdot h^{-1}$)	Noble metal	Ref
Pt@UiO-66-NH_2	λ > 380 nm (300 W)	257.38	Pt	1[1]
MIL-125-NH_2/B-CTF-1	λ > 420 nm (300 W)	360	NO	2[2]
Pt@UiO-66	λ > 420 nm (300 W)	116	Pt	3[3]
Ni_2P@UiO-66-NH_2	λ> 380 nm (300 W)	409	NO	4[4]
Ni1/SnO2/UiO-66-NH_2	λ> 380 nm (300 W)	654	NO	5[5]
Pt/Cu-MIL-125-NH_2	λ > 420 nm (300 W)	490	Pt	6[6]
Pt/PCN-415-NH_2	λ> 380 nm (300 W)	594	Pt	7[7]
Pt/MIL-125-NH_2/$(OH)_2$	λ > 420 nm (300 W)	707	Pt	8[8]
V_2O_5/MIL-125-NH_2	λ> 380 nm (300 W)	298.6	NO	9[9]
TiO_2@ZIF-8	λ> 380 nm (300 W)	254.2	NO	10[10]
MIL-125-NH_2 (facet controlled)	λ > 400 nm (300 W)	60.8	NO	11[11]
CuNPs@d-NH_2-Mil-125	λ > 420 nm (300 W)	1326.55	NO	This work

6. References

1. J. D. Xiao, Q. Shang, Y. Xiong, Q. Zhang, Y. Luo, S. H. Yu and H. L. Jiang, *Angew. Chem., Int. Ed*., 2016, 128, 9535-9539.

2. F. Li, D. Wang, Q. Xing, G. Zhou, S. Liu, Y. Li, L. Zheng, P. Ye and J. Zou, *Applied Catalysis B: Environmental*, 2019, 243, 621-628.

3. J. He, J. Wang, Y. Chen, J. Zhang, D. Duan, Y. Wang and Z. Yan, *Chem Commun*, 2014, 50, 7063-7066.

4. K. Sun, M. Liu, J. Pei, D. Li, C. Ding, K. Wu and H. L. Jiang, *Angew. Chem., Int. Ed*., 2020, 132, 22937-22943.

5. J. Sui, H. Liu, S. Hu, K. Sun, G. Wan, H. Zhou, X. Zheng and H. L. Jiang, *Adv. Mater.*, 2022, 34, 2109203.

6. X. Chen, S. Xiao, H. Wang, W. Wang, Y. Cai, G. Li, M. Qiao, J. Zhu, H. Li, D. Zhang and Y. Lu, *Angew. Chem., Int. Ed*., 2020, 132, 17335-17339.

7. S. Yuan, J. Qin, H. Xu, J. Su, D. Rossi, Y. Chen, L. Zhang, C. Lollar, Q. Wang, H. Jiang, D. H. Son, H. Xu, Z. Huang, X. Zou and H. Zhou, *ACS Centeral Sci*, 2018, 4, 105-111.

8. F. Mohammadnezhad, S. Kampouri, S. K. Wolff, Y. Xu, M. Feyzi, J. Lee, X. Ji and K. C. Stylianou, *ACS Appl. Mater. Inter.*, 2021, 13, 5044-5051.

9. C. Zhang, C. Xie, Y. Gao, X. Tao, C. Ding, F. Fan and H. L. Jiang, *Angew. Chem., Int. Ed*., 2022, 61.

10. M. Zhang, Q. Shang, Y. Wan, Q. Cheng, G. Liao and Z. Pan, *Applied Catalysis B: Environmental*, 2019, 241, 149-158.

11. F. Guo, J. Guo, P. Wang, Y. Kang, Y. Liu, J. Zhao and W. Sun, *Chem Sci*, 2019, 10, 4834-4838.